

Supplementary information for:

**Structure of liquid phase change material AgInSbTe from density
functional/molecular dynamics simulations**

J. Akola^{1,2,3} and R. O. Jones*¹

¹*Institut für Festkörperforschung, Forschungszentrum Jülich, D-52425 Jülich, Germany*

²*Nanoscience Center, Department of Physics,*

P. O. Box 35, FI-40014 University of Jyväskylä, Finland

³*Department of Physics, Tampere University of Technology,*

P. O. Box 692, FI-33101 Tampere, Finland

I. SIMULATION DETAILS

We have used periodic boundary conditions (with a single point ($\mathbf{k}=0$) in the Brillouin zone) and Born-Oppenheimer (BO) molecular dynamics with a Nosé-Hoover thermostat (frequency 800 cm^{-1} , chain length 4).¹ A realistic description of AIST requires that the 4d electrons in Ag and In be treated as “valence” electrons. The localized nature of these orbitals and the use of scalar-relativistic Troullier-Martins pseudopotentials² for all elements require a substantial increase in the plane wave basis. We have used an energy cutoff of 60 Ry, whereas 20 Ry would have been adequate for calculations without the 4d electrons in Ag (valence configuration $4d^{10}5s^1$) and In ($4d^{10}5s^25p^1$). We include non-local core corrections to account for deeper-lying core levels.

II. PAIR DISTRIBUTION FUNCTIONS, COORDINATION NUMBERS

The partial pair distribution functions (PDF) of ℓ -AIST at 850 K are shown in Fig. 1, and the corresponding maxima and partial coordination numbers are listed in Table I. The Sb-Sb and Sb-Te PDF have their first maxima at 3.0 \AA and weak second maxima at 4.2 \AA , which correlate with the distances in the crystalline phase. Sb is the most abundant element and prefers Sb-Sb bonds, while the Te-Te PDF has no maximum before 4.0 \AA . The Sb-Sb, Sb-Te, and Te-Te PDF show deep minima at 5.3 \AA , pronounced maxima at $6.2\text{-}6.3\text{ \AA}$, and damped longer range oscillations above 10 \AA .

The PDF for the minority atoms (dopants) Ag and In are interesting. In has longer bonds ($0.2\text{-}0.3\text{ \AA}$) than Ag, which displaces the maxima in Fig. 1. Sb and Te also prefer $0.1\text{-}0.2\text{ \AA}$ shorter bonds than In (see Table I). The second maximum has merged in the In-Sb and In-Te PDF yielding a shifted and broadened first peak, and we apply a longer bond cutoff (3.5 \AA) for bonds involving In. Both Ag and In prefer Te atoms as their nearest neighbors, but this effect is countered by the much higher Sb concentration. The Ag-Ag, Ag-In, and In-In PDF (Fig. 1) show that Ag-In and In-In bonds are not favored.

The partial coordination numbers are given in Table I for different cutoff distances. We focus on the bold-faced values obtained for 3.3 \AA for bonds not involving In and 3.5 \AA otherwise. The X-In coordination numbers (X is any element) depend only weakly on the choice of cutoff, but there is a significant effect in the In coordination ($n_{\text{In-X}}$). The presence

of small amounts of Ag and In tends to increase the overall coordination. Partial coordination numbers show that Ag and In (and Te) bind mostly with Sb, despite the preference for Te neighbors. Sb-Sb bonds are by far the most common, followed by Sb-Te bonds. Fourfold Sb-Sb₄ (15%) and threefold Te-Sb₃ (21%) are the most common configurations for Sb and Te, respectively.

III. BOND ANGLES

The bond angles have been evaluated using a bond cutoff of 3.3 Å, and the distributions are shown for individual elements [Fig. 2(a), X denotes any atom] and selected configurations [Figs 2(b-c)]. The distributions around Sb and Te are very similar, with maxima at 90°, but no increased contribution for linear configurations near 180°. In has greater weight for angles > 100°, and Ag has two maxima of similar weight [60° (triangles), 90°]. Triangular structures occur, but they are the least common in a monotonically increasing ring distribution.

Fig. 2(b) shows that the most common Sb configurations show similar features. The only exception is the Te-Sb-Te distribution with a distinct maximum at 90° and an increased tendency for nearly linear configurations. Te then appears to increase locally the octahedral nature of the liquid. The bond angles around Ag and In [Fig. 2(c)] support this observation: the angles related to Sb have maxima at 60° (triangles), those related to Te have pronounced peaks around 90°.

IV. CAVITIES AND ATOMIC CHARGES

The cavity analysis has been performed as described in Ref. 3. The system is divided into a cubic mesh with a grid spacing of 0.09 Å, and the points farther from *any* atom than a given cutoff (here 2.8 Å) are selected (*vacancy domains*). Each domain is characterized by the point where the distance to all atoms is a maximum. If there are no maxima closer than the divacancy cutoff (here 2.4 Å), we locate the center of the largest sphere that can be placed inside the cavity and use this point to calculate PDF, including vacancy-vacancy correlations. Around the vacancy domains we construct cells analogous to the Voronoi polyhedra amorphous phases (cf. the Wigner-Seitz cell). This definition and these cutoffs have been used consistently in all our previous work on Ge/Sb/Te alloys.³⁻⁶

Liquid AIST contains only 22 cavities in the 640 atom system, with an average volume of 37.2 \AA^3 . The total volume occupied by the cavities is only 4.2 %, and there are few larger than 100 \AA^3 (divacancies). The cutoff radius (2.8 \AA) is less than typical bond distances in AIST, but larger values would give even less empty space. There is much less free space available in AIST than in Ge/Sb/Te alloys, where volumes up to 19 % were found at high temperatures.⁶ The vacancy PDF show that cavities prefer to have Te and In as neighbors. This is consistent with their smaller short-range coordination.

Integration over the atomic volumes (v_{at} , Voronoi prescription), gives valence (q_{val}) and effective charges (q_{eff}) (see text). Ag attracts electrons to its $5s$ shell and is weakly anionic. Te also gains electrons. Indium is an electron donor (despite the sizable atomic volume), and this is reflected in the In- $5p$ energy eigenvalue, which moves above the Fermi level ($+1.5 \text{ eV}$). The Bader charges show similar trends: Ag and Te are anionic (-0.16 and $-0.47 e$, respectively), and In is cationic ($+0.27 e$).

V. DIFFUSION

The time-dependence of the mean square displacements of atomic types at 850 K and the corresponding linear fits are shown in Fig. 3. Ag is the most mobile element, while diffusion in the other three is rather similar. The modulation of the Ag and In curves reflect the limited statistics available from the small number of atoms (23 and 25, respectively). The diffusion constants (in units of $10^{-5} \text{ cm}^2/\text{s}$) are Ag: 7.33, In: 4.29, Sb: 4.12, and Te: 3.81. If we insert a plausible particle radius of 1.4 \AA in the Stokes-Einstein relation, we obtain a viscosity of 1.1 cP, similar to our estimates for liquid $\text{Ge}_2\text{Sb}_2\text{Te}_5$ (900 K) and $\text{Ge}_8\text{Sb}_2\text{Te}_{11}$ (950 K) with the same particle radius.^{3,6}

¹ G. J. Martyna, M. L. Klein, and M. Tuckerman, *J. Chem. Phys.* **97**, 2635 (1992). The chain modification of the Nosé-Hoover approach leads to a canonical ensemble even in nonergodic systems.

² N. Troullier and J. L. Martins, *Phys. Rev. B* **43**, 1993 (1991).

³ J. Akola and R.O. Jones, *Phys. Rev. B* **76**, 235201 (2007).

⁴ J. Akola and R.O. Jones, *Phys. Rev. Lett.* **100**, 205502 (2008).

⁵ J. Akola and R.O. Jones, J. Phys.: Condens. Matter **20**, 465103 (2008).

⁶ J. Akola and R.O. Jones, Phys. Rev. B **79**, 134118 (2009).

Figures

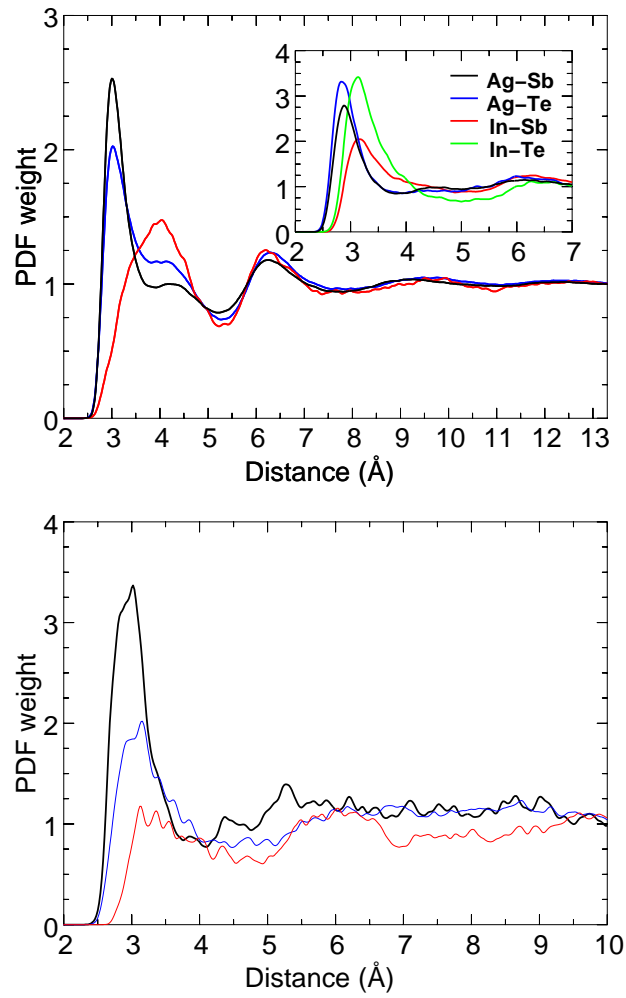


FIG. 1: [Supp. Fig. 1] Partial PDF g_{ij} at 850 K. (a, upper) Thick black: Sb-Sb, blue: Sb-Te, red: Te-Te. Inset: PDF for Sb/Te with Ag/In. (b, lower) Thick black: Ag-Ag, blue: Ag-In, red: In-In.

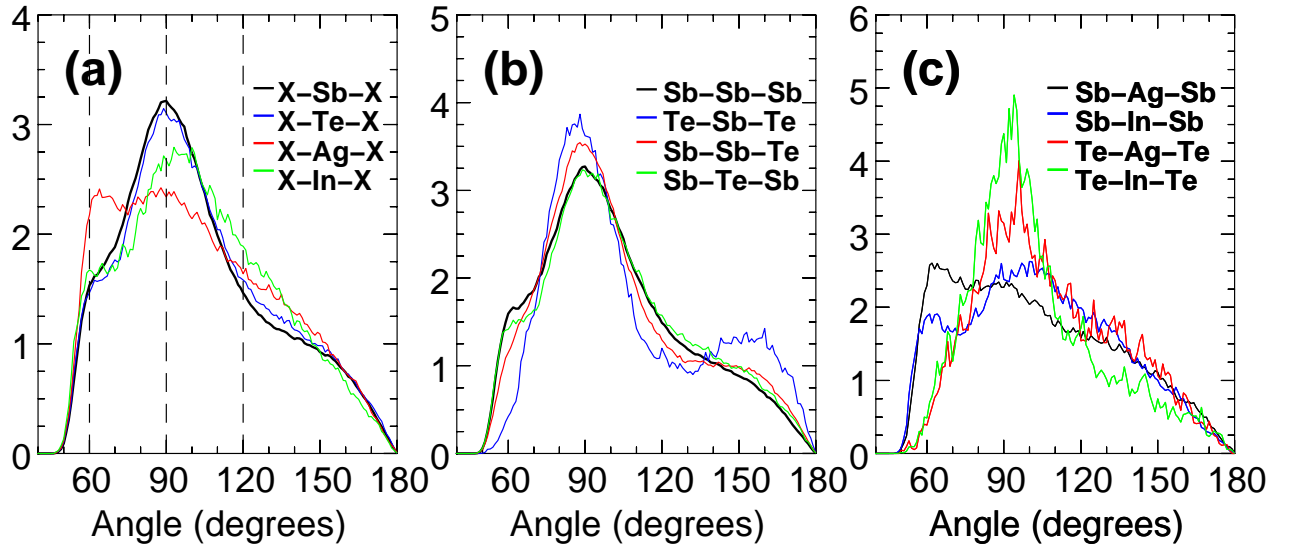


FIG. 2: [Supp. Fig. 2] (a) Bond angles in ℓ -AIST (850 K, X denotes any atom). (b)-(c) Bond angle configurations for bonds $< 3.3 \text{ \AA}$. Note the different scales.

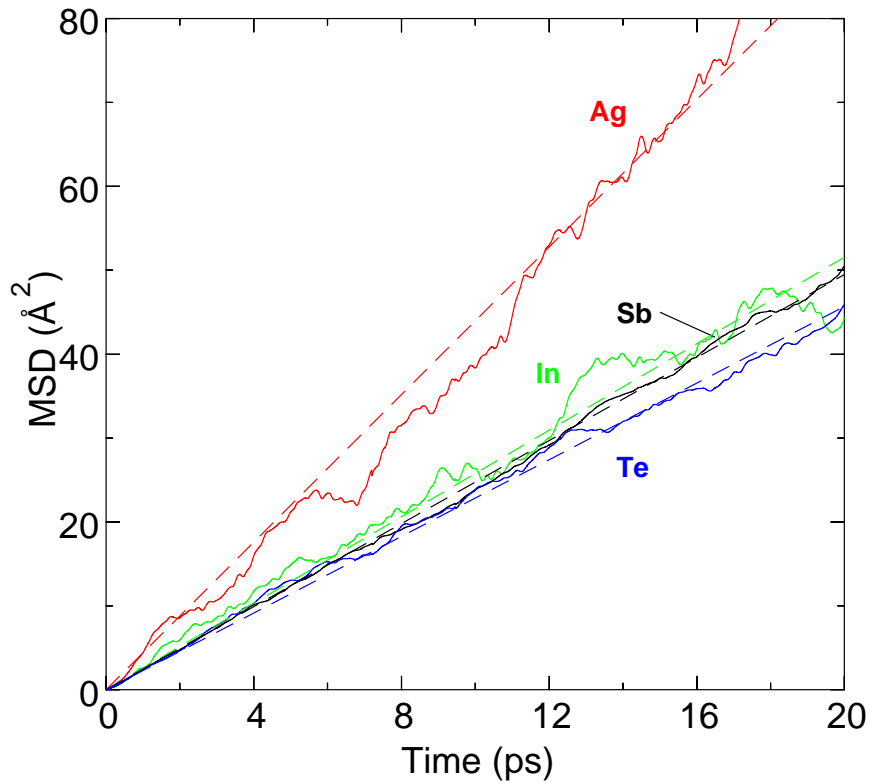


FIG. 3: [Supp. Fig. 3] Mean square displacements of elements in ℓ -AIST at 850 K. Dashed lines: linear fits.

Tables

TABLE I: Bond distances (r_{X-Y} , PDF maximum) and partial coordination numbers (n_{X-Y}) as a function of cutoff distance R_c . The resolution for bond distances is ± 0.05 Å (see Supp. Fig. 1). Bold face values are used in the discussion.

	r_{X-Y}	n_{X-Y} (3.2 Å)	n_{X-Y} (3.3 Å)	n_{X-Y} (3.4 Å)	n_{X-Y} (3.5 Å)
Ag-Ag	2.92	0.21	0.24	0.27	0.29
Ag-In	3.05	0.13	0.16	0.19	0.21
Ag-Sb	2.88	3.48	3.95	4.37	4.77
Ag-Te	2.84	0.98	1.09	1.19	1.28
In-Ag	3.05	0.12	0.15	0.17	0.19
In-In	3.20	0.05	0.06	0.08	0.10
In-Sb	3.15	1.92	2.56	3.15	3.73
In-Te	3.13	0.78	1.01	1.21	1.40
Sb-Ag	2.88	0.17	0.19	0.21	0.23
Sb-In	3.15	0.10	0.13	0.16	0.19
Sb-Sb	3.00	2.72	3.28	3.77	4.22
Sb-Te	3.02	0.53	0.65	0.77	0.89
Te-Ag	2.84	0.20	0.22	0.24	0.26
Te-In	3.13	0.17	0.23	0.27	0.31
Te-Sb	3.02	2.26	2.80	3.32	3.81
Te-Te		0.16	0.23	0.32	0.42